Influence of cation constriction on the ac conductivity dispersion in metaphosphate glasses

D. L. Sidebottom
Department of Chemical and Nuclear Engineering, University of New Mexico, 1001 University Boulevard SE, Albuquerque, New Mexico 87106

(Received 1 October 1999; revised manuscript received 14 January 2000)

The ac conductivity resulting from ion motion in glasses displays a power-law frequency dependence characterized by an exponent $n<1$. Recently, it was suggested that this exponent depends upon the dimensionality of the local cation conduction space, such that n decreases with decreasing dimensionality. Here, I report measurements of the ac conductivity of two metaphosphate glass systems. The first are the superionic glasses formed by doping AgI into $AgPO_3$. The second are the alkali-metal metaphosphate glasses, MPO_3, where $M=$ Li, Na, K, Rb, or Cs. In both glass systems, the conductivity exponent varies with expansion of the phosphate chains which comprise the glass network. In the AgI-doped glasses, n increases with increasing expansion of the network, whereas in the alkali-metal series, n decreases with the expansion. However, when n is considered as a function of the ''constriction'' of the cation (i.e., the cation size relative to the chain separation), this exponent behaves similarly for both glass systems, decreasing with increasing constriction of the cation. This decrease is proposed to result from a reduction in the coordination of the cation's local conduction space caused by increased constriction.

I. INTRODUCTION

The nature of ion transport in amorphous solids is of both practical and academic interest. These materials form a class of solid electrolytes currently under investigation for applications in a variety of electrical devices including batteries, sensors, and electrochromic displays.[1] Physical properties of the disordered state are isotropic and can be manipulated by variations in the chemical composition. So, although most common inorganic glasses are not usually regarded as highly conductive, numerous fast-ion conducting (FIC) glasses, some with ambient dc conductivities comparable to liquid electrolytes, have been reported in the literature.[1–4] Consequently, an enormous range of ion diffusivities is exhibited in glasses and it is of interest on an academic level to try and understand how the chemical and physical structure of the glass influences ion motion.

In traditional oxide glasses, ions (often alkali-metal cations) migrate through a disordered covalently bonded, three-dimensional mesh of network-forming oxides (SiO_2, B_2O_3, etc.). The network contains anionic sites (usually nonbridging oxygen atoms) and voids which can accommodate the cation, as well as doorways through which the cation passes to an adjacent site.[5] The temperature dependence of the dc conductivity is typically Arrhenius and indicates that the transport is a thermally activated process, involving hopping of the cation over local energy barriers.[2,3] These barriers predominantly result from the overlap of neighboring Coulomb wells, but can also include steric barriers associated with the requirement to dilate the network[3,5] between sites in order for the cation to pass.

The influence of network structure on ion transport has been examined both in terms of short-range order (SRO) as well as intermediate-range order (IRO). Jain and co-workers,[6] for example, have investigated the effects of altering the local site structure in sodium silicate glasses through the introduction of trivalent network-forming oxides (B_2O_3 and Al_2O_3). Changes in the activation energy for these modified silicate glasses indicate distinct effects upon ion dynamics due to changes in both the chemical (ionicity) and physical (bond lengths, bond-angle distribution) structure of the network. Pan and Ghosh[7] have also noted variations in ion dynamics due to unique structural transformations occurring in alkali-metal tellurite glasses.

At larger length scales, the presence of intermediate-range order in some glasses has been tied to the occurrence of anomalously high dc conductivity.[8,9] Many of these FIC glasses result when a metal halide is doped into an oxide glass causing systematic increases in the dc conductivity. Neutron-scattering measurements[8] of AgI-doped glasses, for example, reveal the emergence of sharp diffraction peaks in the static structure factor at low wave numbers ($q \approx 0.8\,\text{Å}^{-1}$) with the addition of AgI. The narrow linewidth of these ''prepeaks'' indicates the development of some form of intermediate-range order within the glass with a correlation length of 20–30 Å.[10]

One prominent example of a FIC system that has been extensively investigated[10–17] is the AgI-doped Ag metaphosphate glasses, whose ambient dc conductivity increases by some four orders of magnitude at maximum levels of doping (about 60 mol % AgI) for which a glass can be obtained. Recent neutron scattering and small-angle x-ray scattering (SAXS) of $AgI_x(AgPO_3)_{1-x}$ glasses show little or no prepeak present for the halide-free ($x=0$) base glass, but the development of a prepeak near $q=0.7\,\text{Å}^{-1}$ with the addition of AgI.[10] At higher wave numbers the features of the static structure factor remain essentially unaltered by AgI doping and little effect upon the vibrational modes of the phosphate network is evidenced by Raman scattering.[11] These two observations indicate that AgI is incorporated into interstitial voids surrounding the network,[3,11] as opposed to being incorporated directly into the phosphate network itself. These structural studies resonate well with earlier observations which demonstrated how the dc conductivity[18] and other

physical properties[19] of the AgI-doped $AgPO_3$ glasses, when extrapolated to that of 100% doping, corresponded closely to those of α-AgI, the highly conducting crystalline phase of AgI. Based upon these findings, it was proposed that the addition of AgI leads to the development of AgI-rich microdomains or clusters which percolate through the existing oxide network.[16,20,21] The enhanced conduction in the halide-doped glasses is then seen to result from the greater mobility of the Ag cations which travel along these conduction pathways. However, the recent SAXS investigation of the AgI-doped $AgPO_3$ glasses[10] indicates an alternative interpretation. Although the SAXS does exhibit prepeaks with AgI addition, the intensity of these peaks is insufficient to be the result of AgI clustering. The metaphosphate glass has a linear structure comprised of polymeric chains composed of PO_3 units,[22] and together with reverse Monte Carlo simulations, Wicks and co-workers[10] have argued convincingly that the prepeak is simply a consequence of the lateral expansion of these chains which accompanies the addition of AgI. This expansion leads to greater free volume in the glass and a resulting enhancement of the cation diffusivity. Indeed, a correlation of the dc conductivity to the network expansion has been established for many of the halide-doped FIC's.[23]

However, in addition to the dc conductivity, ion dynamics are also characterized in terms of ionic relaxation displayed by the dielectric response of the glass to a time-dependent electric field. Several years ago, Jonscher[24] noted the universal occurrence of a power-law frequency dependence of the ac conductivity of ionic conductors, including crystalline as well as amorphous materials, of the form $\sigma(f) \approx f^{n_{\rm eff}}$, where the exponent $n_{\rm eff}$ ranged between 0.5 and 1. Experimentally, this exponent varies with temperature, decreasing from a value near unity at low temperatures to $0.6 < n_{\rm eff} < 0.7$ at higher temperature.[25] It has since been recognized[26–28] that the power-law response is in fact composed of two separate contributions, such that

$$\sigma(f) = \sigma_o\{1 + (f/f_o)^n\} + A_{\rm II} f. \tag{1}$$

The first term in Eq. (1) exhibits a strongly activated temperature dependence and represents a contribution to the total ac conductivity due to displacement of the cations; σ_o represents the long-range Fickian diffusion of the cations, while the power law appears to result from localized ($\sim$2 Å) displacements.[29,30] The second term in Eq. (1), which exhibits only a weak temperature dependence, may be a result of low-energy distortions of the anionic network,[27,31,32] and is often referred to as the ''constant loss'' as its approximate linear dependence upon frequency implies a frequency-independent dielectric loss. Whether the constant loss is truly ''constant'' remains an unresolved issue. Some studies claim that the constant loss contribution is precisely linear in frequency,[14] while others[13] have suggested instead that it exhibits a superlinear ($A_{\rm II} f^m$, $m \approx 1.2$) dependence upon the frequency. In either event, due to the differences in their respective temperature dependences, the first term in Eq. (1) dominates the second at high temperatures and indications are that its power-law exponent (n) is neither temperature dependent nor dependent upon the cation concentration.[33,34] Indeed, in temperature and frequency ranges where the constant loss contribution is negligible, the total ac conductivity exhibits scaling[34,35] of the form

$$\frac{\sigma}{\sigma_o} = F_1\left(\frac{f}{f_o}\right). \tag{2}$$

In addition, a remarkable degree of universality in the exponent is observed whereby many glasses, possessing a variety of dissimilar chemical and physical structures, exhibit $n = \frac{2}{3}$.[36] This universality would suggest that specific features of the glass structure, while capable of influencing the dc conduction, are irrelevant to the dispersive behavior of the ac dielectric response.

A survey was recently conducted of the power-law exponent obtained from ac conductivity of ion conductors reported in the literature.[29] In addition to oxide glasses, for which $n = \frac{2}{3}$ was commonly observed, the survey included crystalline conductors such as Na β-alumina (in which the Na ions are constrained to move in the two-dimensional space between alumina planes) and hollandite (for which the ions move within one-dimensional channels) where the smaller exponents $n = 0.58 \pm 0.05$ and $n = 0.3 \pm 0.1$, respectively, were observed. From this study it was proposed that the dispersion in the ac conductivity is influenced by the dimensionality of the ion's conduction space, the exponent decreasing with decreasing dimensionality.

It was also noted that the halide-containing glasses, known for their enhanced dc conductivity, generally display an exponent less than $n = \frac{2}{3}$, suggesting that cations in these systems experience a conduction space of lower dimensionality. A good example is found in the study by Verhoef and den Hartog[37] of LiCl-doped $(Li_2O)_x(B_2O_3)_{1-x}$ glasses where the exponent decreased from $\frac{2}{3}$ in the halide-free glass to about 0.55 in the halide-rich glasses. In the AgI-doped $AgPO_3$ glasses, recent measurements by Le Stanguennec and Elliott[13] indicate an average exponent of only 0.58 ± 0.03, but no clear systematic trend with AgI addition. A tentative interpretation[29] offered for this decreased exponent in the halide-containing glasses is that these glasses might possess extended structure in the form of dendritic conduction pathways with a fractal dimension[38] intermediate between two-dimensional (2D) and three-dimensional (3D). Thus, the issue of whether or not clusters are present in halide-doped glasses resurfaces once more.

In this paper, I report measurements of the conductivity dispersion in the AgI-doped $AgPO_3$ glass system. In contrast with previous measurements which indicated no compositional dependence of the conductivity exponent, a systematic increase in the conductivity exponent from a value typical of 2D conductors to the value of $\frac{2}{3}$ associated[39] with 3D conductors is observed with increasing AgI doping. This finding is inconsistent with the proposed formation of AgI-rich clusters but may be a consequence of expansion of the phosphate network which accompanies the addition of AgI. A companion study of the alkali-metal metaphosphate glasses, MPO_3, with M = Li, Na, K, Rb, and Cs, in which a comparable expansion of the network occurs with increasing alkali-metal size, however, shows the conductivity exponent decreasing from $\frac{2}{3}$ with increasing network expansion.

It is shown that these two contrasting variations of the conductivity dispersion with network expansion can be codi-

TABLE I. Glass properties and results of analyses.

Glass $AgI_x(AgPO_3)_{1-x}$	ρ (g/cm^3)	T_g (K)	n ($\pm$0.005)	E (eV)	d_{ion} (Å)	ρ_{PO_3} (Å^{-3})
$x=0.0$	4.48	445	0.585	0.563	2.52	0.0144
$x=0.1$	4.66	431	0.615	0.533	2.52	0.0131
$x=0.2$	4.90	429	0.640	0.450	2.52	0.0120
$x=0.3$	5.06	394	0.670	0.382	2.52	0.0106
$x=0.4$	5.21	378	0.670	0.341	2.52	0.0091
$x=0.5$	5.43	359	0.650	0.295	2.52	0.0077
$x=0.6$	5.60	338	0.660	0.270	2.52	0.0062
$LiPO_3$	2.35	592	0.670	0.715	1.36	0.0164
$NaPO_3$	2.53	553	0.670	0.732	1.94	0.0149
KPO_3	2.42	533	0.540	0.816	2.66	0.0123
$RbPO_3$	3.06	493	0.545	0.753	2.94	0.0112
$CsPO_3$	3.54	513	0.530	0.621	3.34	0.0100

fied into a consistent variation of the exponent with cation ''constriction'' (i.e., the ratio of the cation diameter to the mean separation distance of the PO_3 chains). For low levels (less than 50%) of constriction, a 3D exponent ($n=\frac{2}{3}$) is observed, while the exponent decreases for increased levels of constriction. This departure of the ion dynamics from 3D in the vicinity of 50% constriction is further supported by far-infrared spectroscopy[40,41] of the cation vibration mode in metaphosphate glasses, whose linewidth narrows substantially when the constriction exceeds about 50%. It is proposed that constriction of the cation between phosphate chains leads to both an increased coordination number of the cation and a reduction of degrees of freedom for local cation displacements, resulting in a lowered effective dimensionality of the cation's local conduction space as well as a decrease in its vibrational density of states.

II. EXPERIMENT

Glasses were prepared from high-purity (>99.9%) nitrates and ammonium dihydrogen phosphate (ADP), $NH_4H_2PO_4$. For the $AgI_x(AgPO_3)_{1-x}$ glasses, appropriate amounts of $AgNO_3$, AgI, and ADP were reacted in a 250-ml Pyrex beaker at approximately 280 °C until gas evolution ceased. The reaction was carefully monitored since the release of gas was rapid (particularly for compositions near $x=0.2$) and could cause the reactants to foam out of the beaker. The resulting product was then melted at approximately 500 °C. The melts ranged in color from orange to dark red, changing to transparent yellow when vitrified. With the exception of the $x=0.6$ samples, which required quenching of the melt between brass plates, glasses were formed by pouring the melt into a brass form and allowing it to cool at room temperature.

For the alkali-metal glass series, appropriate amounts of alkali-metal and ADP were again reacted in a Pyrex beaker at 280 °C until gas evolution ceased. The remaining product was then transferred to a silica crucible and melted at approximately 800 °C and bubbled with dry argon gas for 1 h to minimize the water content. Glass samples were obtained by quenching between preheated brass plates, as it was determined that maintaining the plates near the glass-transition temperature (T_g) produced samples of sufficient stability to be transferred to an annealing oven. As all these glasses are prone to water absorption, they were immediately transferred after annealing to a desiccated container where they were allowed to cool to ambient temperature.

The mass densities of the glasses were measured at room temperature using the Archimedes method with freon as the reference fluid. A small portion of each glass was ground and the glass-transition temperature determined by differential scanning calorimetry. Values of the density and T_g, as well as other quantities, are reported in Table I.

For dielectric measurements, two concentric Ag contacts (about 20 mm diam) were coated onto opposite sides of a glass sample (about 1.5 mm thick) in a dry, argon atmosphere. Isothermal measurements of the complex impedance over a frequency range from less than 1 Hz to approximately 6 MHz were obtained at selected temperature intervals using a commercial (Schlumberger 1260) impedance analyzer. A liquid-nitrogen-cooled cryostat was used for measurements at temperatures below ambient, with a temperature stability of $\pm$0.3 K. For temperatures from ambient to near T_g, a dielectric cell enclosed with a resistive heating element provided temperature stability of $\pm$0.1 K. Samples were purged with dry argon gas during the impedance measurements. Using the geometry of the contacts, measurements of the impedance were converted to ac conductivity and fit by Eq. (1) using a commercial nonlinear least-squares curve-fitting routine.

III. RESULTS

Alkali-metal phosphate glasses are described by the chemical formula $(M_2O)_x(P_2O_5)_{1-x}$, where M is the alkali-metal cation. The structure of vitreous P_2O_5 is composed of P atoms bonded to three neighboring P atoms via bridging oxygens. Addition of M_2O leads to the rupturing of oxygen bonds, which decreases the connectivity of the phosphate network. At the metaphosphate composition ($x=\frac{1}{2}$), the structure, shown schematically in Fig. 1, has an intrinsic polymeric feature.[22] It is comprised of linear chains of repeated PO_3 units. Each PO_3 unit consists of two bridging oxygens and two nonbridging oxygens. The excess negative

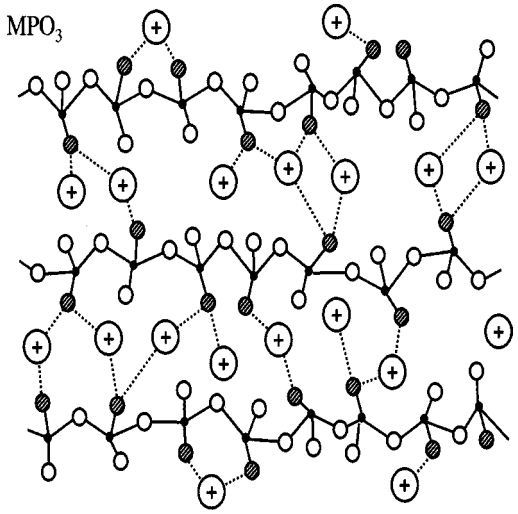

FIG. 1. A schematic representation of the metaphosphate glass structure. Solid circles indicate phosphorus atoms, open circles indicate bridging oxygens, and shaded circles indicate the nonbridging oxygens that are charge compensated by the cations.

charge of the PO_3 unit is distributed evenly between the two nonbridging oxygens and is charge-compensated by the cation which serves to crosslink the PO_3 chains. Earlier work[11] on AgI-doped glasses confirms that the iodine anion is not incorporated into the PO_3 chains, but like the cation resides within the space between chains.

A typical spectrum of the ac conductivity is shown in Fig. 2 for $AgI_{0.4}(AgPO_3)_{0.6}$ measured at 151.8 K. Evident at frequencies below about 100 Hz is the dc conduction region. At higher frequencies, the conductivity increases in a power-law fashion. Included in the figure is the resulting fit of the data of Eq. (1). Despite some systematic variations in the residuals,[42] the quality of the curve fits is considered good since the fit and the data agree to within 5% over the entire

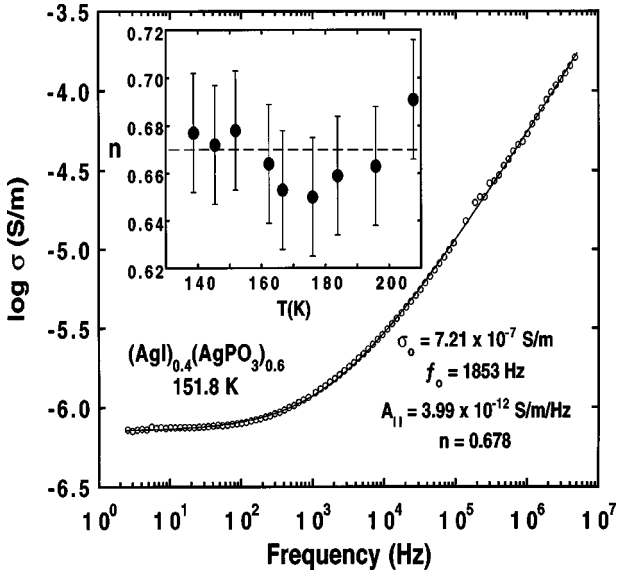

FIG. 2. The ac conductivity of $AgI_{0.4}(AgPO_3)_{0.6}$ at 151.8 K. The solid line is a fit to Eq. (1) with the resulting parameters indicated in the figure. The inset shows the temperature variation of the power-law exponent for this glass composition.

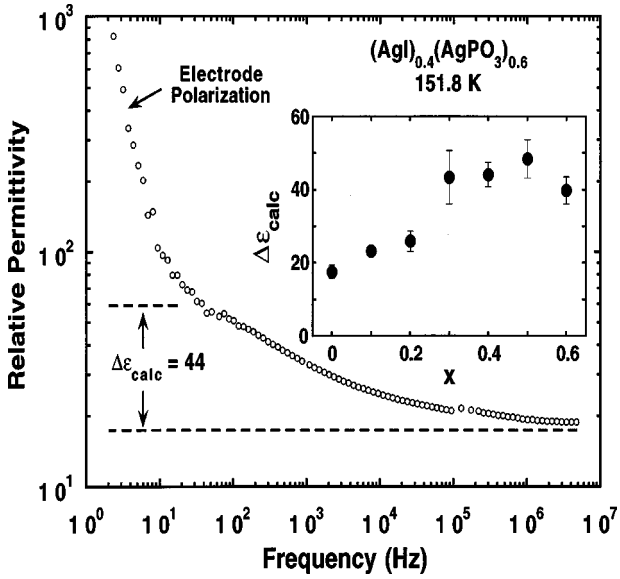

FIG. 3. The ac permittivity of $AgI_{0.4}(AgPO_3)_{0.6}$ at 151.8 K. The dashed lines indicate a shoulder in $\varepsilon(f)$ occurring prior to the onset of electrode polarization, which is consistent with $\Delta\epsilon$ estimated by Eq. (3). The inset shows the variation of $\Delta\epsilon$, as determined from Eq. (3), with increasing AgI addition.

frequency range for all temperatures investigated. Four parameters (σ_o, f_o, n, and $A_{\rm II}$) result from the curve fitting and the error in each varies differently with temperature as a result of the relative location of the relaxation process within the spectrometer's fixed window of frequency.[42–44] The spectrum shown in Fig. 2, for example, is weighted evenly by both the dc conduction and the power-law contribution and the error in all four parameters is comparable. However, at lower temperatures, when much of the dc conduction is situated below 1 Hz, the error in σ_o naturally increases, while at higher temperatures, where the dc conduction extends out to frequencies nearing 1 MHz, the errors in n and $A_{\rm II}$ are naturally increased.[42] Nevertheless, over an intermediate temperature range, the parameters obtained from curve fitting to Eq. (1) are well behaved. The dc conductivity and frequency f_o display approximate Arrhenius temperature variations, while $A_{\rm II}$ [typically $(5\pm3)\times10^{-12}$ S/m/Hz] exhibits no apparent temperature dependence. The conductivity exponent, shown for $AgI_{0.4}(AgPO_3)_{0.6}$ in the inset to Fig. 2, is (within error) temperature independent, consistent with several previous studies[33–35] which have demonstrated scaling of the ac conductivity [see Eq. (2)].

Figure 3 shows the corresponding ac permittivity for $AgI_{0.4}(AgPO_3)_{0.6}$ at 151.8 K. With decreasing frequency, the relative permittivity, $\varepsilon(f)$, increases from the limiting high-frequency dielectric constant, ε_∞ associated with faster polarization mechanisms (electronic, atomic) occurring in the material. At frequencies below about 10 Hz, the permittivity increases considerably. This last increase is due to so-called electrode polarization, in which the long-range displacement of the cations gives rise to charge depletion and accumulation at the respective electrode interfaces and a correspondingly large bulk polarization of the specimen.[45] A slight shoulder is, however, apparent in $\varepsilon(f)$ in the vicinity of 80 Hz. This shoulder indicates the approach of $\varepsilon(f)$ to a limiting low-frequency plateau (ε_s), which would have been vis-

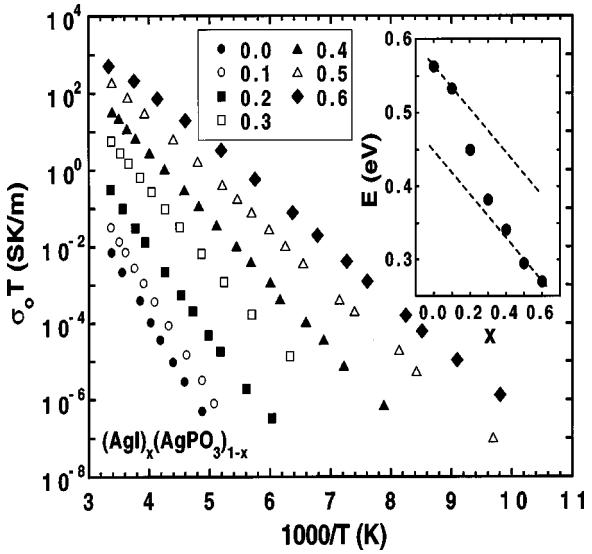

FIG. 4. Arrhenius plot of the dc conductivity (multiplied by the temperature) for various AgI-doped $AgPO_3$ glasses. The inset shows the compositional variation in the activation energy [as defined by Eq. (4)].

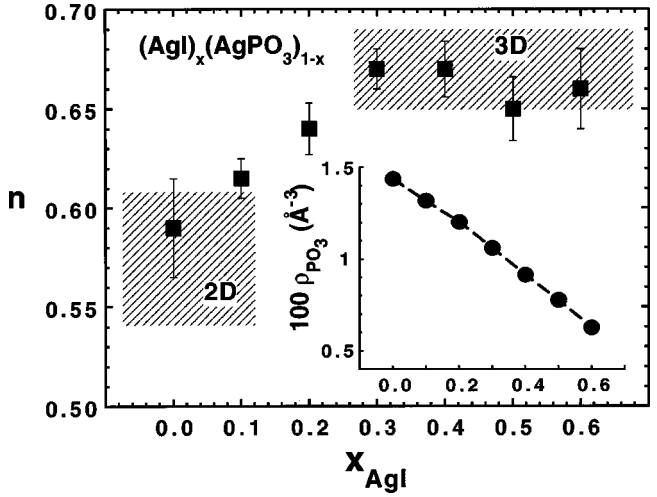

FIG. 5. Variation of the power-law exponent with AgI doping in $AgPO_3$ glasses. The shaded regions indicate upper and lower bounds previously observed for 2D and 3D conductors (Ref. 39). The inset shows the compositional variation of the phosphate chain density.

ible had not the electrode polarization intervened.

Although ε_s cannot be clearly resolved, it can be estimated. Recently,[35] it was proposed that the ac conductivity could be scaled in the manner of Eq. (2) by choosing

$$f_o = \sigma_o / \varepsilon_o \Delta\varepsilon, \tag{3}$$

where $\varepsilon_o = 8.854 \times 10^{-12}$ F/m and $\Delta\varepsilon = \varepsilon_s - \varepsilon_\infty$ is the magnitude of the permittivity change due to ionic relaxation. This relation can be inverted to obtain the estimate $\Delta\varepsilon_{\text{calc}} = 44$ based upon the values of σ_o and f_o required to fit the ac conductivity in Fig. 2. As shown in Fig. 3, this estimate of $\Delta\varepsilon$ agrees favorably with the location of the shoulder discussed above.

In this manner, values of $\Delta\varepsilon$ were determined from σ_o and f_o for all temperatures and AgI concentrations. In most cases, no appreciable temperature dependence was observed. The notable exception is the $x = 0.3$ composition for which $\Delta\varepsilon$ systematically decreased with increasing temperature. The inset to Fig. 3 shows the variation of the mean value of $\Delta\varepsilon$ with AgI addition. Evident in this figure is an apparent transition in $\Delta\varepsilon$ from a value of about 25 for $x < 0.3$ to a value of approximately 45 for $x > 0.3$. Further discussion of scaling in both the conductivity and the permittivity will be addressed in a later section.

In Fig. 4, results for the dc conductivity are plotted in an Arrhenius fashion:

$$\sigma_o T = A \exp(-E/kT). \tag{4}$$

The observed temperature and compositional variation of σ_o is in reasonable agreement with previous studies by Le Stanguennec and Elliott[13] and by Mangion and Johari.[12] The data in Fig. 4 are well approximated by an Arrhenius form [see Eq. (4)], except for the highest doping level where at high temperatures the slope (related to the activation energy E) decreases. This decrease has been observed by others[4] and is considered to be a generic feature of FIC glasses.[46,47] The inset to Fig. 4 shows the compositional variation of the activation energy [defined in Eq. (4)]. With increased doping of AgI into the network, the activation energy decreases and the rate of decrease appears to be maximum in the vicinity of $x = 0.2$.

The variation of the power-law exponent with AgI addition is shown in Fig. 5. Superimposed in the figure are shaded regions which serve to identify the range of n observed previously for 2D crystals and (3D) oxide glasses.[29] The AgI-free, $AgPO_3$ glass displayed the lowest $n \approx 0.59$, oddly suggestive of 2D-like ion dynamics. With addition of AgI up to about 30 mol %, the exponent increases to $n \approx 0.67$, a value typical of many traditional oxide glasses. At higher doping levels, the exponent appears to remain fixed near $n \approx 0.67$. Also plotted in Fig. 5 is the phosphate chain density, $\rho_{PO3} = (1-x) N_A \rho / M_W$, where $N_A = 6.022 \times 10^{23}$, M_W is the molecular weight, and ρ is the mass density. The phosphate density decreases monotonically with increasing AgI addition indicating a continuous expansion of the network. Interestingly, this monotonic expansion is contrasted by the sharp concentration dependence of the exponent, which varies only for doping levels below 30 mol % AgI but remains constant at doping levels from 30 to 60 mol %. The abrupt transition in n around 30 mol % does not correlate with any similarly abrupt changes in the network expansion, but does seem to correlate with the region of rapid increase of the activation energy (see inset to Fig. 4) occurring for doping levels below 30 mol % as well as with the transition in $\Delta\varepsilon$ (see inset to Fig. 3) occurring near 30 mol %.

At this point let us pause to reflect upon the implications of the $n(x)$ variation displayed in Fig. 5. As the figure shows, n increases with AgI and consequently with the emergence of IRO as reported by previous neutron scattering.[10] Early interpretations of the IRO as a result of conduction pathways which percolate within the phosphate network[16,20] seem to conflict with the compositional dependence of n, at least within the context of the proposed dimensionality dependence of this exponent. Presumably such percolated paths would possess some fractal dimensionality lower than 3D and one might have anticipated the exponent to begin with a

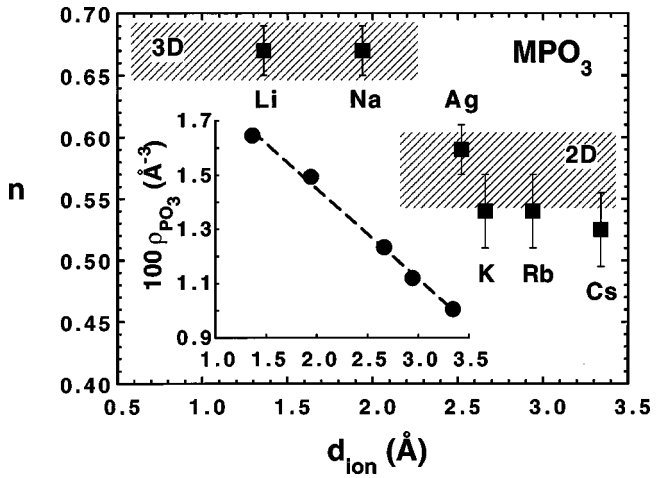

FIG. 6. Variation of the power-law exponent in alkali-metal metaphosphate glasses (and $AgPO_3$) as a function of the diameter of the cation. The shaded regions indicate upper and lower bounds previously observed for 2D and 3D conductors. The inset shows how the phosphate chain density varies with cation diameter.

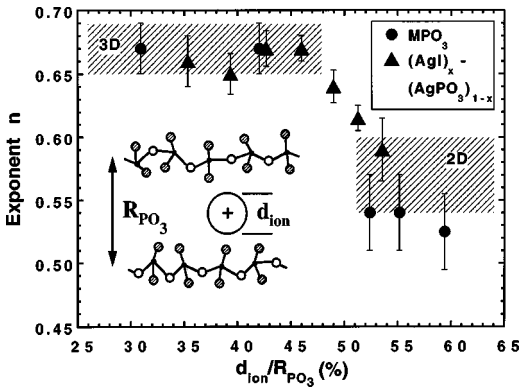

FIG. 7. The power-law exponent for both alkali-metal metaphosphate and AgI-doped $AgPO_3$ glasses plotted as a function of the constriction (see text).

3D-like value ($n \approx \frac{2}{3}$) in the halide-free glass and then decrease with increasing doping. In fact, the trend is just the reverse. Growth of the IRO appears to lead from 2D-like dynamics to 3D-like dynamics.

Recent small-angle x-ray-scattering measurements[10,23] and neutron-diffraction studies[48] likewise concluded that the IRO is not due to cluster formation, but rather is a simple consequence of the lateral expansion of the PO_3 chains. Thus, if the development of IRO is merely a reflection of the expansion of the phosphate network, then the increase in n could be rationalized as a return to 3D-like ion dynamics due to increased local free volume[23] of the cation as the PO_3 chains are spread apart. Then the smaller exponent seen for the (halide-free) $AgPO_3$ glass would indicate that without AgI present the phosphate chains are sufficiently collapsed as to create a local environment for the Ag cation with an effective dimensionality lower than 3D. That is, collapse of the PO_3 chains serves to reduce the number of available conduction pathways in the nearby vicinity.

However, this interpretation for the lowered exponent observed in $AgPO_3$ conflicts with our own previous measurements[27] in other alkali-metal metaphosphate glasses such as $LiPO_3$ and $NaPO_3$, whose chain densities are similar to that of $AgPO_3$, yet whose exponents ($n = \frac{2}{3}$) indicate 3D-like dynamics. One obvious difference between these two alkali-metal metaphosphate glasses and the $AgPO_3$ glass is the size of the cation. The ionic radii[49] of Li and Na (0.68 and 0.97 Å, respectively) are smaller than that (1.26 Å) of Ag. One way then to reconcile this apparent discrepancy in n is to propose that in the $LiPO_3$ and $NaPO_3$ glasses the phosphate chains are insufficiently collapsed relative to the size of the cation for the local cation environment to exhibit a lowered dimensionality. If so, then alkali-metal metaphosphate glasses composed of K, Rb, or Cs with ionic radii (1.33, 1.47, and 1.67 Å, respectively) in excess of that of Ag should exhibit ion dynamics that imitate dimensionalities lower than 3D, like that of $AgPO_3$.

Figure 6 shows the variation of n for the alkali-metal metaphosphate glass series from Li to Cs plotted as a function of the cation diameter, d_{ion}. Once again, shaded regions indicate the approximate bounds previously established[29] for 3D and 2D ion conductors. While alkali-metal cations with $d_{\text{ion}} < 2$ Å exhibit $n \approx \frac{2}{3}$, larger alkali-metal cations indeed show a substantially smaller $n \approx 0.54$, just lower than that typical of 2D conductors. Interestingly, this decrease in n with increasing alkali-metal size occurs despite the accompanying expansion of the PO_3 network, as indicated in the inset to Fig. 6.

Although it seems contradictory that n increases with PO_3 expansion in the $AgI_x(AgPO_3)_{1-x}$ glasses (Fig. 5), but decreases with expansion in the alkali-metal series (Fig. 6), the coordination of the cation's local conduction space is not determined by the chain spacing alone. One must also consider variations of the cation size. For the alkali-metal series the network expansion is accompanied by increasing cation size, while for the $AgI_x(AgPO_3)_{1-x}$ series, the cation size remains fixed. Hence, if the power-law dispersion is related to coordination of the cation's local conduction space, then that coordination may be better expressed in terms *relative* to the size of the cation.

To test this, exponents for both the alkali-metal metaphosphate and $AgI_x(AgPO_3)_{1-x}$ glass systems are plotted together in Fig. 7 as a function of the cation ''constriction.'' This constriction is defined by the ratio of the cation diameter to the average PO_3 chain separation, R_{PO3} [taken to be $2(\pi l \rho_{\text{PO3}})^{-1/2}$, where the length of a PO_3 unit along the chain, l, is estimated as 4 Å]. Plotted in this manner, a common variation of the conductivity dispersion is one in which n exhibits a 3D-like exponent ($n \approx 0.67$) for levels of constriction less than about 50%, but decreases to values corresponding to a lower effective dimensionality for higher levels of constriction. The simple interpretation of this finding is that if the cation possesses sufficient local free volume that it can be displaced normal to the neighboring chains by at least one diameter, then in addition to allowed displacements tangential to the chains, its localized dynamics behave in a 3D-like manner. On the other hand, at higher levels of constriction, collapse of the chains about the cation reduces the degree of freedom associated with displacements normal to the chains. This reduction in the cation's degrees of freedom is also reflected in changes that occur in the cation's coordination sphere. In the glasses with low constriction (e.g., $LiPO_3$ and $NaPO_3$) the cation is coordinated with between

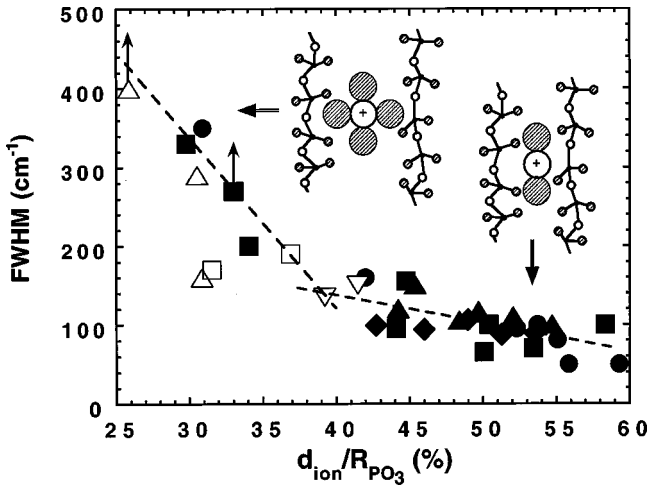

FIG. 8. The linewidth of the cation vibration mode (Ref. 41) plotted as a function of the cation constriction. Glasses include M_2O:P_2O_5 (circles), MO:P_2O_5 (squares), M_2O_3:P_2O_5 (triangles), and MO_2:P_2O_5 (inverted triangles). Also included are data (Ref. 53) for $AgI_x(AgPO_3)_{1-x}$ at $x=0$, 0.1, 0.2, 0.3, and 0.4 (diamonds). Open symbols indicate where the mass density was unavailable and instead approximated as 3 g/cm^3.

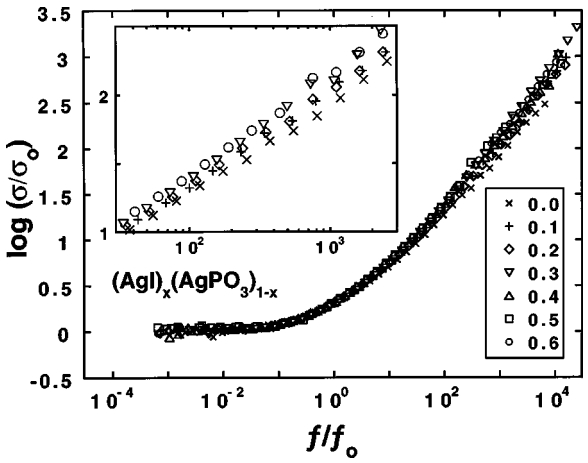

FIG. 9. The ac conductivity of $AgI_x(AgPO_3)_{1-x}$ glasses scaled according to Eq. (2). Each individual spectrum has $\sigma_0 \approx 10^{-7}$ S/m. The inset shows an expanded view showing how the low AgI-containing compositions fail to collapse to a common curve.

two and four oxygen atoms,[50,51] while this coordination number increases to between five and seven for the more highly constricted glasses.[50,52]

Furthermore, the influence of constriction is indicated by the known narrowing of the cation-anion vibrational mode observed by far-infrared spectroscopy[40,41,53] in a variety of metaphosphate glasses. Far-infrared studies have reported an absorption maximum in the 100–400-cm^{-1} energy range whose position varies inversely with the square root of the cation mass, and has been assigned to vibrations of the cation ''rattling'' within an oxygen cage.[41] In the alkali-metal metaphosphate series, this mode narrows with increasing alkali-metal mass and/or size. In Fig. 8, the reported[41] full width at half maximum for the cation vibration mode is plotted as a function of the constriction. In addition to the alkali-metal metaphosphate, several other metaphosphate glasses composed of cations of higher charge state (+2, +3, and +4) for which the mass density of the glass is known or could be estimated[54] are included. As seen in the figure, the cation vibrational mode narrows rapidly with increasing constriction but generally is greater than 100 cm^{-1} for constrictions less than about 40%. For constrictions larger than 40%, the full width at half maximum (FWHM) remains less than 100 cm^{-1} and exhibits a more gradual decrease with increasing constriction. It is quite plausible then that this narrowing is yet another manifestation of the constriction, which diminishes modes of oscillation normal to the PO_3 chains and in so doing reduces the vibrational density of states.

One may question the labeling of the constricted metaphosphate glasses as ''2D'' since this 2D feature, unlike that in alkali-metal β-alumina, does not persist indefinitely through the phosphate network, but exists only within the local vicinity of the cation. The term ''dimensionality'' as applied here to a cation's local environment is meant to reflect the coordination of available conduction space, that is, the set of possible locations to which the cation can be displaced. This is appropriate since the dispersion itself appears to be of a similar localized nature, representing a mean displacement of the cation of only about 2 Å.[30,35] It should be noted that such localized motion is also exemplified in models like that of Funke,[55,56] in which the dispersion results from rapid, correlated (backward/forward) hopping of the cation between its initial site and neighboring sites, as well as in Monte Carlo simulations on percolated lattices where variations in the local conduction pathways play an important role.[57]

One concern for the proposed interpretation of these changes in the conductivity dispersion in AgI-doped $AgPO_3$ is the contradictory behavior indicated in the study by Verhoef and den Hartog[37] of LiCl-doped lithium borate glasses. There, they observed the conductivity exponent decrease with LiCl addition, suggesting a decreasing dimensionality that would accord with clustering models. On the other hand, this same glass system was included in the survey by Swenson and Borjesson,[23] which showed how its dc conductivity increased with expansion of the borate network in the same manner as several other halide-doped FIC glasses, including the AgI-doped $AgPO_3$ glasses. In our own preliminary investigation of LiCl-doped lithium borate glasses, we have yet to observe any systematic deviation of n from $\frac{2}{3}$ for LiCl levels comparable to those reported by Verhoef and den Hartog.[37] Clearly, the LiCl-doped borate glasses will require further study.

Before concluding, one must address how the present work differs with previous similar investigations. Of the three previous studies[12–14] of the ac ionic relaxation in $AgI_x(AgPO_3)_{1-x}$ glasses, two have explicitly considered the power-law dispersion seen in the ac conductivity. A study by Roling[14] focused upon the scaling behavior of $\sigma(f)$. In that study, the ac conductivity of four glass compositions ($x=0.1$, 0.3, 0.4, and 0.55), scaled in accordance with Eq. (2), was shown to collapse to a common curve, implying that n is independent of AgI content, in contradiction to the present finding. In Fig. 9, a similar attempt is made to scale the ac conductivity from the present study. Although spectra at AgI contents of 30 mol % or more do appear to collapse to a common curve, spectra at lower AgI contents systematically

lie below this curve, consistent with the lower exponent we observed in our curve fitting. This inability to scale $\sigma(f)$ is not contingent upon how the scaling parameters (σ_0, f_0) are determined, but stems from changes occurring in the scaling exponent. The failure to scale is subtle since the variation in n across the entire composition range is not substantial. Thus it seems the scaling result of Roling is most likely a fortuitous consequence of the compositions selected in their scaling analysis, which favor those glasses with AgI contents of 30 mol % and greater.

In the study by Le Stanguennec and Elliott,[13] emphasis was placed upon the existence of the two contributions to the ac conductivity discussed earlier with regards to Eq. (1). In their study, the ac conductivity was described by a variant of Eq. (1) in which the second term (linear in frequency) is replaced by a power law of the form $A_{\mathrm{II}} f^m$, where m is near unity. They report no systematic composition dependence of either power-law exponent with $n \approx 0.58$ and $m \approx 1.2$. In the present analysis, m has been fixed at unity. This reduces the number of free parameters in the fit and avoids trouble with the natural tendency for two power laws to ''couple.'' That is, unless a substantial range of $\sigma(f)$ is available over which the two power laws can be unambiguously distinguished, the two exponents (n,m) can take on a range of values, inversely related, which produce nearly indistinguishable fits. The potential for inverse coupling of n and m may account for the slightly smaller average n (≈ 0.58) reported by Le Stanguennec and Elliott as compared with the present study, where the value of n averaged over all compositions is 0.64. The primary goal here is to accurately determine the exponent of the ionic contribution. One method to circumvent this problem is to fit data using only the first term in Eq. (1) with n replaced by n_{eff}, an effective exponent which incorporates both power laws. Then, as a function of temperature, n_{eff} decreases with increasing temperature from a value near unity to a plateau ($n_{\mathrm{eff}}=n$) at higher temperatures where the ionic contribution dominates the total $\sigma(f)$. Performing this sort of analysis resulted in the same values of n (within error) as those shown in Fig. 5 obtained by fitting to Eq. (1).

Finally, I return to the issue of scaling of ac dielectric data. In an earlier work,[35] it was proposed that the ac conductivity could be scaled in a manner described by Eq. (2) with f_0 given by Eq. (3). In that work, several examples were provided for which electrode polarization effects[45] were less problematic and values of $\Delta\varepsilon$ could be extracted from $\varepsilon(f)$ with reasonable accuracy. As one can see from the example in Fig. 3, such a direct determination of $\Delta\varepsilon$ from the data is not feasible in the current situation. Nevertheless, a test of the scaling given in Eq. (3) can be made by examining the complimentary scaling of the ac permittivity.

Since the ac conductivity and the ac permittivity are conjugate pairs related through the Kramer-Kronig relations, the scaling behavior of one should apply equally to the other. Here I examine the dielectric spectra for $AgI_{0.3}(AgPO_3)_{0.7}$, since this composition exhibited temperature-dependent variations in $\Delta\varepsilon = \sigma_0 / f_0 \varepsilon_0$. Figure 10 shows the conductivity measured at five temperatures scaled in the manner of Eq. (2), where f_0 is provided by the curve fitting of Eq. (1). Also shown is the corresponding permittivity, $\varepsilon(f/f_0)$. Clearly, the $\varepsilon(f/f_0)$ do not collapse to a common curve, but appear to be spaced vertically with decreasing temperature. From the

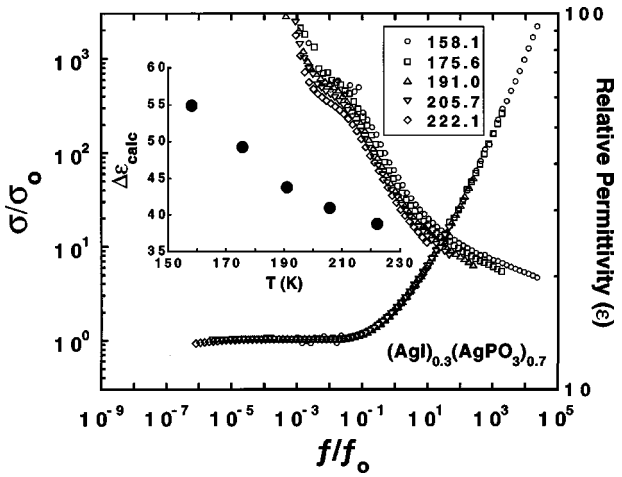

FIG. 10. The ac conductivity of $AgI_{0.3}(AgPO_3)_{0.7}$ measured at five temperatures (in degrees Kelvin) scaled according to Eq. (2) together with the ac permittivity displayed on the same frequency scale. The inset shows the temperature variation of $\Delta\varepsilon$ as calculated from Eq. (3).

values of σ_0 and f_0 used to scale $\sigma(f)$, $\Delta\varepsilon$ can be estimated from Eq. (3) and the result, shown in the inset to Fig. 10, varies systematically with temperature in the same manner as the vertical spacing of $\varepsilon(f/f_0)$ seen in the figure.

In order to scale the permittivity, two operations must be performed.[58] First, the ionic contribution must be isolated by subtracting the high-frequency dielectric constant (ε_∞). Second, the result should, in a manner symmetrical with Eq. (2) for scaling the conductivity, be divided by the magnitude of the permittivity increase ($\Delta\varepsilon$). As Fig. 11 reveals, these two operations do indeed result in collapse of the ac permittivity to a common scaling curve of the form

$$\frac{\varepsilon-\varepsilon_\infty}{\Delta\varepsilon} = F_2\left(\frac{f}{f_0}\right). \tag{5}$$

Since the $\Delta\varepsilon$ required to complete the vertical scaling of permittivity coincides with that determined from Eq. (3), this

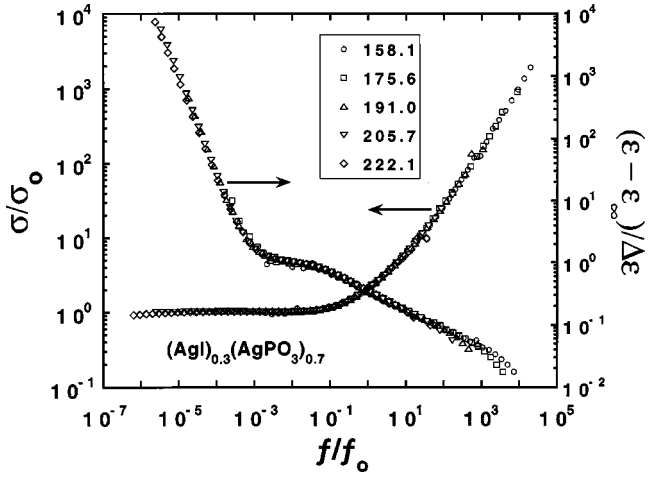

FIG. 11. The ac conductivity and ac permittivity of $AgI_{0.3}(AgPO_3)_{0.7}$ scaled according to Eq. (2) and Eq. (5), respectively, with f_0 given by Eq. (3).

equation together with Eq. (2) and Eq. (3) form a complete expression of the scaling in the ac dielectric response of such ion-conducting materials.

IV. CONCLUSION

The origin of the power-law dispersion of the ac conductivity in ionic materials remains elusive, but the present study of metaphosphate glasses with their unique linear chain structure offers some insight. Investigation of the FIC AgI-doped $AgPO_3$ glasses reveals a compositional variation of the dispersion wherein the power-law exponent increases with AgI addition up to about 30 mol %, contrary to previous studies. This power-law exponent has recently been correlated to the dimensionality of the cation conduction space, in the sense that n generally decreases with decreasing dimensionality. Although the FIC properties of the AgI-doped $AgPO_3$ glasses have been interpreted in the past as resulting from formation of halide-rich clusters, the increase of n with AgI addition suggests an increasing dimensionality which is inconsistent with cluster models. Instead the increase in n is better understood as a consequence of expansion of the PO_3 network, as recently proposed by others,[10] which serves to increase the free volume of the local cation environment. When the phosphate chains are sufficiently expanded relative to the cation size, the coordination of the local cation conduction space assumes the characteristics of a higher-dimensional space and the ac conductivity displays power-law dispersion with $n \approx \frac{2}{3}$. But when the chains are collapsed relative to the cation size, this local environment becomes constricted, predominantly in the direction normal to adjacent chains, leading to a reduced coordination of the conduction space and a corresponding decrease in n. This interpretation is further supported by changes in the vibrational density of state of the cation. A correlation between the ac conductivity dispersion and the cation's vibrational motion is observed in which the vibrational density of states narrows appreciably in conjunction with collapse of the chains about the cation.

ACKNOWLEDGMENTS

The author is grateful to Dr. A. Matic and Dr. J. Swenson for stimulating discussion, and to Professor R. Brow for helpful suggestions. This work was supported by the U.S. Department of Energy, Division of Basic Energy Science (Grant No. DE-FG03-98ER45696).

[1] C. A. Angell, Annu. Rev. Phys. Chem. **43**, 693 (1992).
[2] C. A. Angell, Solid State Ionics **9&10**, 3 (1983).
[3] S. W. Martin, J. Am. Ceram. Soc. **74**, 1767 (1991).
[4] J. Kincs and S. W. Martin, Phys. Rev. Lett. **76**, 70 (1996).
[5] O. L. Anderson and D. A. Stuart, J. Am. Ceram. Soc. **37**, 573 (1954).
[6] C. H. Hsieh and H. Jain, J. Non-Cryst. Solids **183**, 1 (1995).
[7] A. Pan and A. Ghosh, Phys. Rev. B **60**, 3224 (1999); **59**, 899 (1999).
[8] L. Borjesson, L. M. Torell, U. Dahlborg, and W. S. Howells, Phys. Rev. B **39**, 3404 (1989).
[9] J. Swenson, L. Borjesson, and W. S. Howells, Phys. Rev. B **57**, 13 514 (1998).
[10] J. D. Wicks, L. Borjesson, G. Bushnell-Wye, W. S. Howells, and R. L. McGreevy, Phys. Rev. Lett. **74**, 726 (1995).
[11] J. P. Malugani and M. Mercier, Solid State Ionics **13**, 293 (1984).
[12] M. B. M. Mangion and G. P. Johari, Phys. Chem. Glasses **29**, 225 (1988).
[13] M. Le Stanguennec and S. R. Elliott, Solid State Ionics **73**, 199 (1994).
[14] B. Roling, M. D. Ingram, M. Lange, and K. Funke, Phys. Rev. B **56**, 13 619 (1997).
[15] J. W. Zwanziger, K. K. Olsen, and S. L. Tagg, Phys. Rev. B **47**, 14 618 (1993).
[16] P. Benassi, A. Fontana, and P. A. M. Rodrigues, Phys. Rev. B **43**, 1756 (1991).
[17] C. Liu and C. A. Angell, J. Non-Cryst. Solids **83**, 162 (1986).
[18] J. P. Malugani, G. Robert, and R. Mercier, Mater. Res. Bull. **15**, 715 (1980).
[19] L. Borjesson and L. M. Torell, Phys. Lett. **107A**, 190 (1985).
[20] M. Tachez, M. Mercier, J. P. Malugani, and A. J. Dianoux, Solid State Ionics **20**, 93 (1986).
[21] M. Mangion and G. P. Johari, Phys. Rev. B **36**, 8845 (1987).
[22] S. W. Martin, Eur. J. Solid State Inorg. Chem. **28**, 163 (1991).
[23] J. Swenson and L. Borjesson, Phys. Rev. Lett. **77**, 3569 (1996).
[24] A. K. Jonscher, Nature (London) **267**, 673 (1977).
[25] W. K. Lee, J. F. Liu, and A. S. Nowick, Phys. Rev. Lett. **67**, 1559 (1991).
[26] S. R. Elliott, Solid State Ionics **70/71**, 27 (1994).
[27] D. L. Sidebottom, P. F. Green, and R. K. Brow, Phys. Rev. Lett. **74**, 5068 (1995).
[28] A. S. Nowick, A. V. Vaysleyb, and I. Kuskowsky, Phys. Rev. B **58**, 8398 (1998).
[29] D. L. Sidebottom, Phys. Rev. Lett. **83**, 983 (1999).
[30] B. Roling, C. Martiny, and K. Funke, J. Non-Cryst. Solids **249**, 201 (1999).
[31] G. Balzer-Jollenbeck, O. Kanert, H. Jain, and K. L. Ngai, Phys. Rev. B **39**, 6071 (1989).
[32] K. L. Ngai and C. T. Moynihan, Mater. Res. Bull. **23**, 51 (1998).
[33] D. L. Sidebottom, P. F. Green, and R. K. Brow, Phys. Rev. B **56**, 170 (1997).
[34] B. Roling, A. Happe, K. Funke, and M. D. Ingram, Phys. Rev. Lett. **78**, 2160 (1997).
[35] D. L. Sidebottom, Phys. Rev. Lett. **82**, 3653 (1999).
[36] H. Kahnt, Ber. Bunsenges. Phys. Chem. **95**, 1021 (1991).
[37] A. H. Verhoef and H. W. den Hartog, Solid State Ionics **68**, 305 (1994).
[38] D. Stauffer, *Introduction to Percolation Theory* (Taylor and Francis, Philadelphia, 1985).
[39] Although the precise dimensionality is not known (and may be less than 3), the convention of associating 3D-like dynamics with the oxide glasses was established previously in Ref. 29.
[40] G. J. Exarhos, P. J. Miller, and W. M. Risen, Jr., J. Chem. Phys. **60**, 4145 (1974).
[41] B. N. Nelson and G. J. Exarhos, J. Chem. Phys. **71**, 2739 (1979).
[42] D. L. Sidebottom, J. Non-Cryst. Solids **244**, 223 (1999).

[43] H. Jain and C. H. Hsieh, J. Non-Cryst. Solids **172-174**, 1408 (1994).
[44] J. R. Macdonald, J. Non-Cryst. Solids **210**, 70 (1997).
[45] J. H. Ambrus, C. T. Moynihan, and P. B. Macedo, J. Phys. Chem. **76**, 3287 (1972).
[46] K. Ngai and A. K. Rizos, Phys. Rev. Lett. **76**, 1296 (1996).
[47] P. Maass, M. Meyer, A. Bunde, and W. Dieterich, Phys. Rev. Lett. **77**, 1528 (1996).
[48] J. H. Lee and S. R. Elliott, Phys. Rev. B **54**, 12 109 (1996).
[49] *CRC Handbook of Chemistry and Physics*, edited by R. C. Weast, M. J. Astle, and W. H. Beyer (CRC, Boca Raton, FL, 1983).
[50] J. Swenson, A. Matic, A. Brodin, L. Borjesson, and W. S. Howells, Phys. Rev. B **58**, 11 331 (1998).
[51] K. Suzuki and M. Ueno, J. Phys. (Paris), Colloq. **48**, C8-261 (1985).
[52] U. Hoppe, G. Walter, D. Stachel, and A. C. Hannon, Ber. Bunsenges. Phys. Chem. **100**, 1569 (1996).
[53] J. Hudgens (private communication).
[54] O. V. Mazurin, M. V. Streltsina, and T. P. Shvaiko-Shvaikovskaya, *Handbook of Glass Data* (Elsevier, New York, 1985), Vol. 15B.
[55] K. Funke and I. Riess, Z. Phys. Chem., Neue Folge **140**, 217 (1984).
[56] K. Funke, Prog. Solid State Chem. **22**, 111 (1993).
[57] P. Maass, M. Meyer, and A. Bunde, Phys. Rev. B **51**, 8164 (1995).
[58] D. L. Sidebottom and J. Zhang (unpublished).